

Compatibility between itinerant synaptic receptors and stable postsynaptic structure

Ken Sekimoto^{*1,*2} and Antoine Triller^{*3}

^{*1} *Matières et Systèmes Complexes, CNRS-UMR7057, Université Paris 7, France*

^{*2} *Gulliver, CNRS-UMR7083, ESPCI, Paris, France*

^{*3} *INSERM, U789, Biologie Cellulaire de la Synapse N&P,
Ecole Normale Supérieure, Paris, France*

The density of synaptic receptors in front of presynaptic release sites is stabilized in the presence of scaffold proteins, but the receptors and scaffold molecules have local exchanges with characteristic times shorter than that of the receptor-scaffold assembly. We propose a mesoscopic model to account for the regulation of the local density of receptors as quasi-equilibrium. It is based on two zones (synaptic and extrasynaptic) and multi-layer (membrane, sub-membrane and cytoplasmic) topological organization. The model includes the balance of chemical potentials associated with the receptor and scaffold protein concentrations in the various compartments. The model shows highly cooperative behavior including a “phase change” resulting in the formation of well-defined post-synaptic domains. This study provides theoretical tools to approach the complex issue of synaptic stability at the synapse, where receptors are transiently trapped yet rapidly diffuse laterally on the plasma membrane.

PACS numbers: 87.16.dr, 87.16.A-, 87.15.R-

I. INTRODUCTION - BIOLOGICAL BACKGROUND AND PROBLEM

A large body of structural data has shown that synaptic receptors accumulate in the postsynaptic density (PSD). The classic static view of receptor distribution was challenged a few years ago by the evidence that receptor numbers at synapses are tuned during regulation of synaptic strength (reviewed in Refs [1, 2, 3]). This is now considered one of the molecular bases of synaptic plasticity. Synaptic plasticity is one of the most commonly used concepts to explain the capacity of the brain to adapt to external and internal conditions and to modify the properties of neuronal networks in relation to development and learning. The tuning of receptor numbers has led to the important notion

of receptor flux into and out of synapses, both at rest and during plasticity. It has prompted the development of dynamic real-time imaging approaches in living neurons, such as video-microscopy of green fluorescent protein (GFP)-tagged receptors, to go beyond the fixed snapshots given by immuno-cytochemistry. However, these multimolecular approaches have limits: Although they can detect receptor fluxes (e.g. using fluorescence recovery after photobleaching, FRAP), in basal conditions when synaptic receptor numbers remain constant overall, they cannot monitor minute exchanges between compartments. The advent of single molecule imaging techniques now enables measurement of individual receptor movements in identified sub-membrane compartments, and reveals the inhomogeneities and new physical parameters important for the understanding of *receptor trafficking*. The chemical approach is appropriate to further clarify the interplay between the constituent molecules of the postsynaptic molecular assembly. Our theoretical model is intended to present a realistic view of how those molecules behave both individually and collectively.

The synapse as a multimolecular assembly should be viewed as a construction where the constituent elements are characterized by dwell time (local turnover). In other words, the synapse as a whole and the constituent elements have specific characteristic times. This view is not unique to the synapse, but is now well accepted for structures like actin and microtubules with well-known tread-milling behavior or the turnover of ATPase molecular motors during cell motility[4] and in intracellular trafficking [5]. Theoretical frameworks accounting for the dynamics of these structures have been proposed and have allowed the development of a new experimental paradigm [6, 7, 8]. Such a theoretical approach has been lacking for the postsynaptic membrane. The structures of the synapse that are unified for excitatory and inhibitory contacts have been extensively studied during the two last decades. The recent development of dynamic methods and real-time imaging, e.g. single-particle tracking (SPT) and FRAP [9], has allowed molecular behavior to be deciphered on a short time-scale (msec). Therefore, it is now possible to propose new explanations of how the stability and plasticity of synapses can be accounted for by interactions between molecules present in various compartments such as the extracellular protein domains in the presynaptic membrane, the plasma membrane (receptors and associated molecules), the cytosol (scaffold molecules) and extracellular matrix.

The preferential and specific localizations of receptors at synapses result from their interactions with sub-membrane scaffold proteins. Comparison with the neuro-muscular junction encouraged the postulate that scaffold proteins are involved in the so-called *stabilization* and *increased density*

of the receptors at synapses [9]. These two concepts, often unduly mixed, were extended to most central synapses and believed to be the heart of synapse-specific receptor localization. This was reinforced by the discovery and characterization of numerous scaffold molecules interacting with inhibitory [10] or excitatory receptors [11]. These structural and biochemical observations have perpetuated the notion that at steady state receptors are fixed at synapses and that this accounts for their density. Although electrophysiology has long since provided evidence for the existence of extrasynaptic receptors [12], they were often thought to constitute a pool distinct from synaptic receptors. More importantly, their physiological roles have been limited to activation by spillover of neurotransmitter outside the synaptic cleft during massive release [13, 14, 15, 16] or during glutamate release by neighboring glia [17]. The notion that extrasynaptic and synaptic receptors are separate entities was reinforced by the fact that some receptor isoforms have specific sub-cellular distributions.

Interactions between pre- and post-synaptic elements are also important in determining not only the localization of synaptic contacts but also their excitatory or inhibitory nature [18, 19]. The key molecules in this “balancing act” are postsynaptic neuroligins, which interact with the β -neurexins, which are themselves located in the presynaptic release active zone. On the postsynaptic side, they are likely to bind to scaffold proteins. Therefore, the postsynaptic neuroligins provide the localization signal for the specific accumulation of given receptors at inhibitory or excitatory synapses. Without entering into detail, one of the most interesting features of this system is that these molecules, which induce either excitatory or inhibitory synapses, underpin the control of excitation-inhibition balance. Other adhesive molecules such as N-cadherins are involved in the homomeric interaction linking the presynaptic and postsynaptic membranes.

The generic organization of the synapse is given in Fig. 1. Receptors are indirectly linked to the presynaptic terminal buttons *via* scaffold proteins and trans-synaptic homophilic or heterophilic molecular interactions. We seek to link this topological organization to the movements of both receptors and scaffold proteins. This minimal picture holds for both excitatory and inhibitory synapses. There are more species of receptors and scaffold proteins at a given synapse than shown in the figure, and the molecular organization can be rather complex. In this study we have homogenized synaptic structure to account for diffusing receptors and scaffold proteins as a global entity. In fact the dynamic and static aspects of a system can be viewed differently depending on the resolution of experimental observation or model description. At the molecular level, thermal agitations cause both the spatial Brownian motion and chemical fluctuations of con-

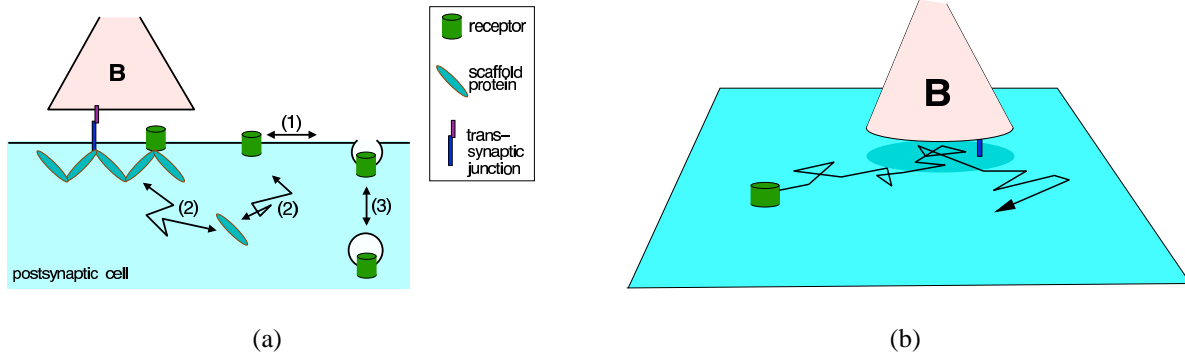


FIG. 1: (Color online) (a) Generic description of molecular mechanisms involved in the accumulation of receptors in front of terminal buttons (B). The arrow indicates: (1) the membrane diffusion of receptors; (2) the cytoplasmic diffusion of scaffold proteins and their binding to receptors; and (3) the endocytosis/exocytosis of receptors.

(b) Schematic representation of the diffusive motion of receptors at the cell surface [20].

stituent molecules, added to which are the driving forces due to interaction among the molecules. On a mesoscopic level, the molecules are observable exclusively through their densities, and the thermal agitations are perceptible only as diffusion. Therefore, once the diffusion has reached a stationary or quasi-stationary state, the stability of a spatial density profile on a mesoscopic level can *coexist* with the microscopic fluctuations of constituent molecules mentioned above. This fact, which was recognized in the late 19th century in the context of gas kinetics, can be applied to many other problems where we discuss a phenomenon on two different scales. In particular, there are cases where the stationary state can be achieved with negligible net fluxes of energy and material species, a situation called *quasi-equilibrium*. Such situations are characterized by the balance of chemical potentials of molecules both in space and in the chemical species in which the molecules move around. The peculiarity of the (quasi-)equilibrium state compared with other steady states is that the balance conditions of chemical potentials, called the detailed balance condition in statistical physics, contain *no* kinetic parameters [21]. In the present paper, we explore a mesoscopic description of the quasi-equilibrium in the postsynaptic molecular architecture. The rationale and consequences of the model are explained in general terms more accessible to biologists in Appendix C. The complexity of the synapse can in fact be accounted for by extending the number of zones and layers, as will be defined in Fig. 4. We neglect the interaction between scaffold proteins and actin cytoskeletons (see also § II C). It has been shown that the postsynaptic scaffolds of excitatory and inhibitory synapses in hippocampal neurons maintain their core

components independent of actin filaments and microtubules. [22].

II. PHYSICAL INTERPRETATION

A. Reciprocal stabilization

The general picture that we propose in the present paper is that receptors accumulating in front of the presynaptic release site are “stabilized” by scaffolding molecules. The locus of the synaptic contact is supposed to be “determined” by homophilic or heterophilic interactions between the pre- and post-synaptic membranes. The stabilizing mechanism of the receptor density through the interaction with sub-membrane substances has also been explored in the context of cell adhesion[23, 24] or of cellular recognition[25], or the polymer adsorption by surfactants[26]. A distinct feature of the present case of synaptic assembly is its reciprocal nature: The sub-membrane substances (scaffold proteins) are also assembled by the molecules on the membrane (receptors), while in the former cases it was large objects like colloids [23], vesicles [24], micron-size particles [25] or polymers [26] that interact with many molecules on the membrane.

B. Decoupling of kinetics from energetics in quasi-equilibrium

In the context of the problem and the minimal model of quasi-equilibrium presented above, we will briefly describe the *separation* of kinetic aspects from static ones mentioned in the introduction (see Fig. 2). The conclusion is that, in the quasi-equilibrium situation, the accumulation of receptor density under the synapse should not be ascribed to kinetic mechanisms such as small mobility of receptors inside a synaptic zone, but to the static aspect of molecular interactions.

Fig. 2 (a) shows a potential profile for a receptor diffusing on the membrane with higher barriers inside than outside synapses. Obstacles within synapses create potential barriers which modify the kinetics (reduced diffusion), but do not necessarily create higher receptor density at steady state. One can show by a simple calculation that if the rightward and leftward transition rates across each barrier are symmetric, the probability of finding the receptor is homogeneously distributed in the steady state. By contrast, in Fig. 2(b) the mean level of the potential valley is lowered within synapses, but the potential barriers are unchanged there. As a consequence, with potential barriers of the same height inside and outside synapses, receptors diffuse equally fast in extrasynaptic and

synaptic regions, although the density is increased in the latter. This simplistic schematic representation again emphasizes that postsynaptic accumulation and diffusivity are two independent physical characteristics. We note that, as this separation is strictly valid only at equilibrium, it is not a mere temporal analogue of the concept of the compatibility between microscopic fluctuations and mesoscopic steady state mentioned in the previous section. Below we will identify the time-window where we can apply approximately the theoretical framework of quasi-equilibrium to the processes of receptors and scaffold proteins.

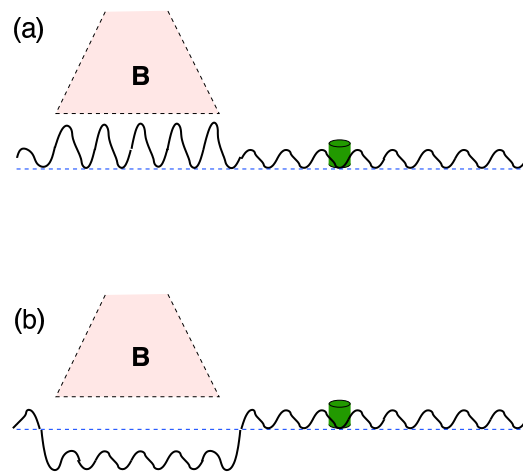


FIG. 2: (Color online) Kinetic and energetic components involved in receptor mobility and accumulation; (a,b) Potential energy profile (thick wavy lines) for a receptor (green object). Note its alterations below the presynaptic bouton (B), illustrating two extreme situations. Compared to extrasynaptic membrane, the energy barrier can be higher (a) or the energy level lower (b). The consequences are that (a) the diffusion is slowed down beneath the synaptic bouton but the density of receptors can be identical at synaptic and extrasynaptic membrane in the steady state; (b) that the diffusion coefficients can be identical within the two zones but receptor density is higher beneath the synaptic bouton. Experimental data (accumulation of receptors and lower diffusion coefficient) [20] indicate that a combination of the two is responsible for accumulation of receptors.

C. Summary of time scales and justification of quasi-equilibrium treatment

Neurotransmitter receptors undergo both lateral diffusion on the plasma membrane and cycling through exo-/endo-cytosis between the plasma membrane and cytoplasmic vesicles. We postulate two characteristic time scales:

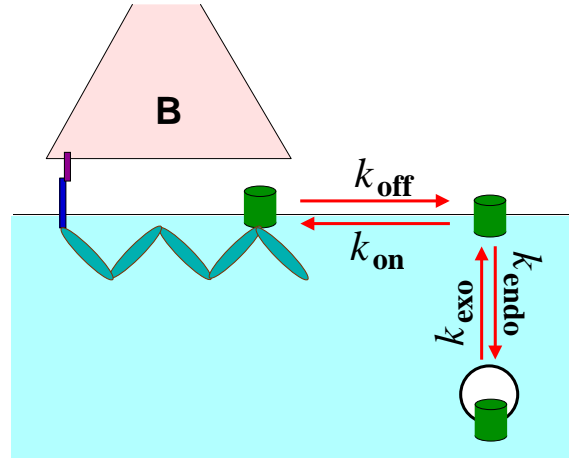


FIG. 3: (Color online) Kinetic parameters and cellular biology of receptors. Exo/endocytosis and synaptic to extrasynaptic transfer are characterized by specific rate constants, $k_{\text{endo/exo}} \ll k_{\text{on/off}}$. The half-life of receptors in the plasma membrane (on the order of tens of minutes to half a day) and the dwell time of receptors at synapses are given in terms of these parameters.

$\tau_{R,\text{eq}}$: (quasi-)equilibration time of the receptors on the postsynaptic cell membrane

$\tau_{R,\text{cyc}}$: recycling time of receptors related to endocytosis and exocytosis

The rate of receptor exchanges k_{on} and k_{off} , k_{endo} and k_{exo} allows the computation of $\tau_{R,\text{eq}} = (k_{\text{on}} + k_{\text{off}})^{-1}$ and $\tau_{R,\text{cyc}} = (k_{\text{endo}} + k_{\text{exo}})^{-1}$, respectively (Fig. 3). Experimental evidence indicates that $\tau_{R,\text{eq}}$ ranges from tens of seconds to minutes, and $\tau_{R,\text{cyc}}$ ranges from tens of minutes to about half a day [27, 28]. The scaffold proteins also experience movements between the plasma membrane periphery and the bulk cytoplasm. Furthermore, local amounts of scaffold proteins in the bulk cytoplasm are regulated by means of expression/degradation, or by transport-associated compartmentalization. Here again, we can postulate two characteristic time-scales:

$\tau_{s,\text{eq}}$: (quasi-)equilibration time for the migration of scaffold proteins

$\tau_{s,\text{cyc}}$: recycling time related to the synthesis and degradation of scaffold proteins

Experimental evidence indicates that $\tau_{s,\text{eq}}$ is of the order of minutes to tens of minutes [29, 30], while $\tau_{s,\text{cyc}}$ is likely to be several hours.

We can thus estimate the time window for quasi-equilibrium as between minutes and hours. That is, when (i) both the number of receptors on the plasma membrane and the density of scaffold proteins in the cytoplasm remain almost constant, while (ii) the membrane diffusion of receptors

and the cytoplasmic diffusion of scaffold proteins have reached equilibrium. We therefore focus on the time window Δt for observation/description with the following limits:

$$\max\{\tau_{R,eq}, \tau_{s,eq}\} \lesssim \Delta t \lesssim \min\{\tau_{R,cyc}, \tau_{s,cyc}\}. \quad (1)$$

and develop in the following section a quasi-equilibrium model using assumptions (i) and (ii).

One might ask if the actin cytoskeleton forms a network underneath the scaffold proteins and works as a frozen heterogeneous background. The recent FRAP analyses, however, have shown that, about 85 % of actins in dendritic spines are turned over within 44 seconds[31], and also the turnover of α -actinin (passive actin-binding protein) is more rapid than that of PSD-95, a scaffold protein of the excitatory synapse [30]. Therefore, within the time window Δt defined above, we assume that the actin cytoskeleton is a fluid-like background and ignore it in our minimal model.

III. MESOSCOPIC MODEL AND PHASE-EQUILIBRIA

A. Spatial compartments and density variables

The quasi-equilibrium defined above will be assumed in the homogenized schema of the post-synaptic cell (Fig.4 (a)). We assume three layers along the vertical direction to the membrane: The outmost layer is the *membrane layer* with all the receptors and other trans-membrane signaling proteins (see below). The intermediate and *sub-membrane layer* (a few nanometers) constitute the cytoplasmic volume where scaffold proteins interact with receptors and other trans-membrane molecules (e.g. adhesion molecules). The innermost layer is the *bulk cytoplasm*, which is the reservoir of scaffold proteins that swap with the sub-membrane layer.

Laterally, we define *synaptic* (superscript: z) and *extrasynaptic* (superscript: x) zones. This partition can be justified since the time-scale of modeling is greater than the equilibration time of both receptors and scaffold proteins. However, we have neglected possible mesoscopic substructures within the synaptic zone, a point to be considered in future investigations. The reservoir of scaffold proteins is common to these two zones. Within these five compartments, we attribute densities to membrane receptors and sub-membrane scaffold proteins as follows, see Fig.4(a).

$\sigma_R^{(z)}$ and $\sigma_R^{(x)}$: number of receptors (suffix: R) per surface area (areal density) in the synaptic and extrasynaptic zones, respectively,

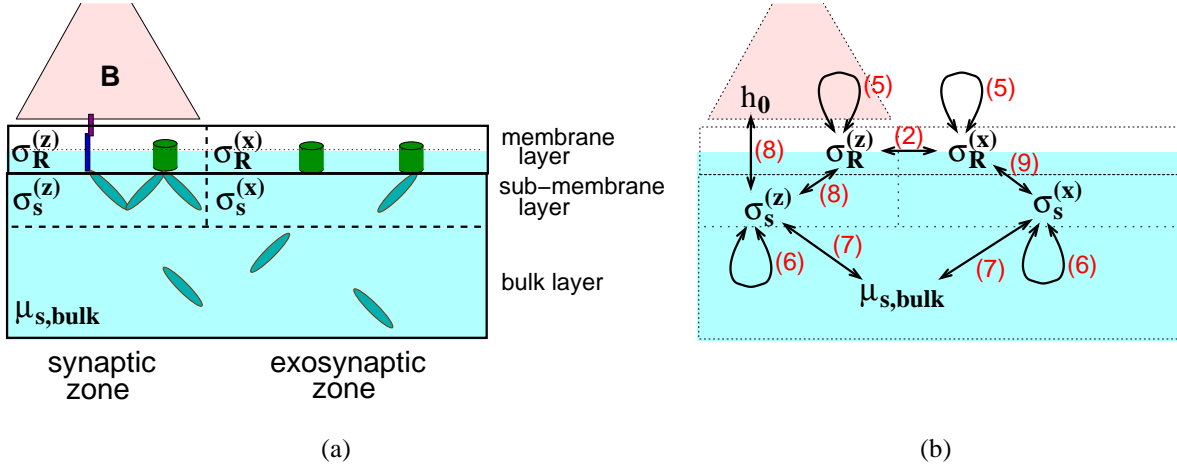


FIG. 4: (Color online) (a) Three-layer, two-zone model: The model assumes a three-layer partition of the postsynaptic cell: *membrane layer*, *sub-membrane layer* and *bulk layer*. In the first two layers, we establish a spatial partition with two zones: a synaptic (z) and an extrasynaptic (x) zone, where the areal densities (σ) are used as variables, and receptors (**R**) and scaffold proteins (**s**) are indicated as suffixes. In the bulk layer, the density of scaffold proteins corresponds to chemical potential, $\mu_{s,bulk}$. The receptors can diffuse within the membrane layer, and the scaffold proteins diffuse among the zones in both the sub-membrane layer and the bulk layer.

(b) Correlations among molecules: The arrows indicate the molecular correlations taken into account in the present model. The numbers like (2) etc. correspond to those of equations in the text.

$\sigma_s^{(z)}$ and $\sigma_s^{(x)}$: number of scaffold proteins (suffix: s) per surface area (areal density) in the sub-membrane synaptic and extrasynaptic zones, respectively.

Here superscripts ^(z) [^(x)] denote the quantities associated with the synaptic zone [extrasynaptic zone], respectively.

The total number of receptors on the membrane is constant within the time-scale of modeling, and is expressed by

$$N_R = A^{(z)}\sigma_R^{(z)} + A^{(x)}\sigma_R^{(x)} = \text{constant}, \quad (2)$$

where N_R is the total number of membrane receptors, and $A^{(z)}$ and $A^{(x)}$ are the surface areas of the synaptic zone and extrasynaptic zone, respectively. Experimental data indicate that receptors can be exchanged between synaptic sites [20] and, therefore, the membrane can be considered as a global field where synaptic contact introduces a singularity allowing for the local accumulation of the constituent elements of the postsynaptic machinery. Thus, each synapse behaves as a donor or acceptor of molecules.

As for the mechanism determining the spatial extension of the PSD, one might consider a physical mechanism which minimizes the free energies due to surface (peripheral) contribution and the bulk (areal) contribution. A possible origin is entropic, that is, the steric repulsion among molecules reflecting their three-dimensional geometrical arrangement. Such situation is well exemplified in recent work on syntaxin 1 clusters [32]. However, the actual size of the synaptic density matches the size of the presynaptic active zone. We therefore will not elaborate on this issue and simply assume here that the size of PSD is determined externally. The size of the PSD is likely to be correlated with the number of scaffold proteins. The total number of scaffold proteins in the sub-membrane layer can fluctuate despite a constant density in the layer of bulk cytoplasm. As a consequence,, scaffold protein chemical potential is an important parameter (see the text below and Eq.7).

B. Construction of free energy

The observed densities of constituent molecules in the quasi-equilibrium state correspond to the maximum probability of realization. Following Gibbs' statistical mechanics, this probability is given by the Boltzmann factor, $e^{-G/k_B T}$, where G is a pertinent (Gibbs) free energy function for the whole system. The maximum of this factor defines the (Boltzmann) equilibrium. G is the sum of the contributions from each compartment,

$$G = A^{(z)} g^{(z)} + A^{(x)} g^{(x)}, \quad (3)$$

where $g^{(z)}$ [$g^{(x)}$] are the *free energies* per unit area of the membrane in the synaptic [extrasynaptic] zone, respectively. The variables of these free energies will be introduced below. Experimental data suggest that, in our minimal model, $g^{(\alpha)}$ ($\alpha = z$ or x) can be constructed from the following components :

$$g^{(\alpha)} = g_{\text{mem}}^{(\alpha)} + g_{\text{sub}}^{(\alpha)} + g_{\text{bulk}}^{(\alpha)} + g_{\text{mem-sub}}^{(\alpha)}. \quad (4)$$

Here the first three terms denote the contributions from each layer, i.e. the membrane layer (mem), sub-membrane layer (sub) and bulk layer (bulk), respectively, and the last term is the key term representing the interactions between the first two layers. The biological counterparts of $g_{\text{mem}}^{(\alpha)}$, $g_{\text{sub}}^{(\alpha)}$, $g_{\text{bulk}}^{(\alpha)}$ and $g_{\text{mem-sub}}^{(\alpha)}$ correspond to the free energy associated with receptors in the plasma membrane ($g_{\text{mem}}^{(\alpha)}$), scaffold proteins in the sub-membrane layer (i.e., scaffold proteins in the bulk cytoplasm in relation to specific domains) ($g_{\text{sub}}^{(\alpha)}$), scaffold proteins in the rest of the bulk cytoplasm ($g_{\text{bulk}}^{(\alpha)}$), and

scaffold-transmembrane protein interactions ($g_{\text{mem-sub}}^{(\alpha)}$), respectively. We detail these terms below (see also Fig. 4(b)).

Membrane layer :

The term $g_{\text{mem}}^{(\alpha)}$ contains the density of the receptors in the corresponding zone, $\sigma_{\text{R}}^{(\alpha)}$, and we assume no direct binding interaction between receptors *except for* the lateral steric exclusion:

$$g_{\text{mem}}^{(\alpha)}(\sigma_{\text{R}}^{(\alpha)}) = k_{\text{B}}T \left[\sigma_{\text{R}}^{(\alpha)} \log \frac{\sigma_{\text{R}}^{(\alpha)}}{\sigma_{\text{R}0}} + (\sigma_{\text{R}0} - \sigma_{\text{R}}^{(\alpha)}) \log \frac{\sigma_{\text{R}0} - \sigma_{\text{R}}^{(\alpha)}}{\sigma_{\text{R}0}} \right], \quad (5)$$

where $\sigma_{\text{R}0}$ is the saturation density, which we assumed to be common to the two zones. Eq.5 was deduced from the factor $e^{-(A^{(\alpha)}g_{\text{mem}}^{(\alpha)} + A^{(\alpha)}g_{\text{mem}}^{(\alpha)})/k_{\text{B}}T}$, which gives the combinatorial number for spatial distribution of the receptors on the membrane. This equation Eq.5 establishes the relationship between the geometrical distribution of individual receptors and the (free) energy of a collection of receptors.

Sub-membrane layer :

The term $g_{\text{sub}}^{(\alpha)}$, which has the same form as in Eq.5, accounts for scaffold proteins. In addition to geometrical volume exclusion, this equation takes into account a specific attractive interaction among scaffold proteins ($U(\sigma_{\text{s}}^{(\alpha)})$).

$$g_{\text{sub}}^{(\alpha)}(\sigma_{\text{s}}^{(\alpha)}) = k_{\text{B}}T \left[\sigma_{\text{s}}^{(\alpha)} \log \frac{\sigma_{\text{s}}^{(\alpha)}}{\sigma_{\text{s}0}} + (\sigma_{\text{s}0} - \sigma_{\text{s}}^{(\alpha)}) \log \frac{\sigma_{\text{s}0} - \sigma_{\text{s}}^{(\alpha)}}{\sigma_{\text{s}0}} \right] + U(\sigma_{\text{s}}^{(\alpha)}), \quad (6)$$

where $\sigma_{\text{s}0}$ is the saturation (areal) density of the scaffold proteins. The last term $U_{\text{s}}(\sigma_{\text{s}}^{(\alpha)})$ representing the non-combinatorial part of the free energy includes the entropic cost of confinement (U_1), the mutual attraction among the scaffold proteins (U_2) and the specific saturation effect among them (U_4), which imposes a smaller limiting value than $\sigma_{\text{s}0}$. Recent molecular studies [33] on the scaffold protein for the inhibitory synapse (gephyrin) have identified trimerization and dimerization domains. They may be responsible for the hexagonal oligomerization of the postsynaptic scaffold organization [34]. The attraction by $U_2 (< 0)$ and non-steric saturation $U_4 (> 0)$ reflects these findings. We therefore propose for $U_{\text{s}}(\sigma_{\text{s}}^{(\alpha)})$ the following function: $U_{\text{s}}(\sigma_{\text{s}}) = U_1\sigma_{\text{s}} + U_2\sigma_{\text{s}}^2 + U_4\sigma_{\text{s}}^4$, with the coefficients $U_1 > 0$, $U_2 < 0$ and $U_4 > 0$. see Fig. 5(top). The most important term is U_2 (the attractive term) because U_1 can be included as a shift of the chemical potential of the reservoir (see below), while the last term U_4 acts effectively as steric repulsion.

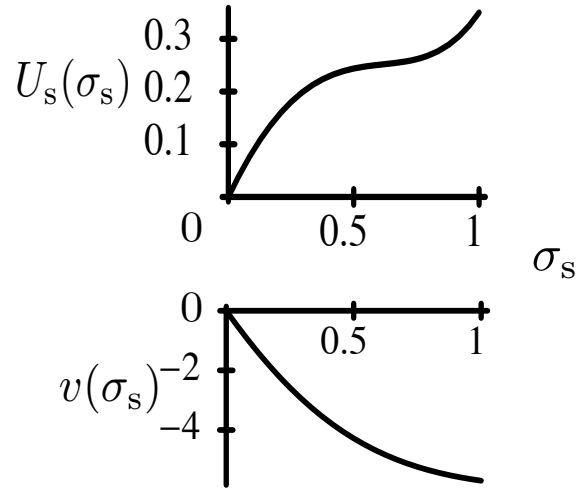


FIG. 5: $U_s(\sigma_s)$ vs σ_s (top) and $v(\sigma_s)$ vs σ_s (bottom).

Bulk layer :

The term $g_{\text{bulk}}^{(\alpha)}$ represents the free energy associated with scaffold proteins of the bulk cytoplasm. It is characterized only by the chemical potential of these scaffold proteins, which we denote by $\mu_{\text{s,bulk}}$. Although there is a single contribution to G from the scaffold proteins in the bulk cytoplasm, $(-\mu_{\text{s,bulk}})(A^{(z)}\sigma_s^{(z)} + A^{(x)}\sigma_s^{(x)})$, it can be separated in two parts, i.e. $A^{(z)}g_{\text{bulk}}^{(z)}$ and $A^{(x)}g_{\text{bulk}}^{(x)}$, linked to synaptic (z) and extrasynaptic (x) zones, respectively:

$$g_{\text{bulk}}^{(\alpha)}(\sigma_s^{(\alpha)}) = -\mu_{\text{s,bulk}} \sigma_s^{(\alpha)}. \quad (7)$$

In biological terms, an increase in scaffold proteins in the bulk cytoplasm will increase $\mu_{\text{s,bulk}}$, and therefore the capacity of these proteins to be involved in the clustering of postsynaptic receptors.

Membrane/sub-membrane interface :

The formal description of the interactions between compartments must take into account their interfaces. The interface for molecular interactions sets a discontinuity in the molecular organization of the synapse. Depending on the zone, the interaction free energy, $g_{\text{mem-sub}}^{(\alpha)}$ contains one or two contributions: The interaction between membrane receptor and scaffold protein, and additional interaction between scaffold protein and a trans-membrane protein involved in pre-to-postsynaptic signaling for the localization of the contact. The latter contribution is denominated h_0 , and behaves as an attracting field (See Fig. 2(b)), introducing

a local energetic component recruiting scaffold proteins. The interaction free energy at the synapse is now expressed as:

$$g_{\text{mem-sub}}^{(z)}(\sigma_{\text{R}}^{(z)}, \sigma_{\text{s}}^{(z)}, h_0) = \sigma_{\text{R}}^{(z)} v(\sigma_{\text{s}}^{(z)}) - h_0 \sigma_{\text{s}}^{(z)} \quad (8)$$

and outside of synapse as:

$$g_{\text{mem-sub}}^{(x)}(\sigma_{\text{R}}^{(x)}, \sigma_{\text{s}}^{(x)}) = \sigma_{\text{R}}^{(x)} v(\sigma_{\text{s}}^{(x)}). \quad (9)$$

The first term in both equations represents the interaction between membrane receptor and scaffold protein, and depends on receptor and scaffold protein density. $v(\sigma_{\text{s}}^{(x)})$ should reflect (i) linearity in the dilute regime, (ii) curvature for intermediate regime, and (iii) saturation at high concentration regime. The saturation is related to the steric hindrance of molecules and to the number of binding sites available on a receptor for interaction with scaffold proteins. We have tried the following two forms: (1) $v(\sigma_{\text{s}}) = v_{\text{f}}[1 - e^{-v_1(\sigma_{\text{s}}/\sigma_{\text{s}0}) - v_2(\sigma_{\text{s}}/\sigma_{\text{s}0})^2}]$ (see Fig.5 (bottom)) and (2) $v(\sigma_{\text{s}}) = v_{\text{f}}[v_1(\sigma_{\text{s}}/\sigma_{\text{s}0}) - \tilde{v}_2(\sigma_{\text{s}}/\sigma_{\text{s}0})^2]$, where $v_{\text{f}}(< 0)$ corresponds to the specific attractive power between the two group of molecules, while $v_1(> 0)$ and $v_2(> 0)$ or $\tilde{v}_2(> 0)$ realize the above three features, (i)-(iii). The overall characteristics of $v(\sigma_{\text{s}})$ in (2) are similar to Fig.5 (bottom) for $0 < \sigma_{\text{s}}/\sigma_{\text{s}0} < 1$. It turns out that the qualitative results of the numerical analyses are robust against the choice between the types (1) and (2), and we will present below the results for case (1) only. That we have retained only the linear dependency on $\sigma_{\text{R}}^{(x)}$ is based on the observation that the number of receptors at a synaptic site is usually well below the stoichiometric limit determined by the number of underlying scaffold proteins. The number of receptors present in a PSD is below 100 for excitatory [35] and inhibitory [36] synapses. In contrast, the number of scaffolding molecules such as PSD-95 in excitatory postsynaptic differentiations is about 300 [37]. Therefore, the ratio of receptor to scaffold binding sites is likely to be below 50%. The second term of Eq.8 represents the positive bias for the scaffolding molecules due to the transsynaptic signal, and therefore exists only in the synaptic zone. This signal is carried through the interaction between the transmembrane molecules. The range of h_0 is such that this bias is reversible and does not exceed too much the order of $k_{\text{B}}T$.

In biological terms, the expression of the free energies for the membrane/sub-membrane interface accounts for the network of molecular interactions between presynaptic terminals through

adhesion (h_0), scaffold proteins ($\sigma_s^{(z)}$) and receptors ($\sigma_R^{(z)}$). This will now allow us to sum the contributions from the layers and their interfaces to obtain the free energy G , which will be used in the next section to establish the conditions of the quasi-equilibrium.

C. Phase equilibria

What we will denominate below as the *phase* is any realization of physical states that corresponds to the minimum of the model free energy function (“Landau function”) with respect to its variables specifying physical states. In the present model the variables are the densities, $\{\sigma_R^{(z)}, \sigma_R^{(x)}, \sigma_s^{(z)}, \sigma_s^{(x)}\}$. In this case, a phase can represent spatially heterogeneous distributions of membrane receptors and sub-membrane scaffold proteins. The *phase change* is then the phenomenon where the distribution of these molecules changes in a discontinuous manner as some model parameters are changed continuously across a transition point.

The phase change can be strictly defined and realized only if the system that a model represents is infinitely large. Otherwise, the thermal fluctuations in the vicinity of the transition point may cause the temporal switching between one phase to the other. Therefore, characteristic switching time depends on the system size. The present model deals with synaptic boutons, which are on a mesoscopic scale. In each synaptic bouton the PSD contains receptors and scaffold proteins of the order of tens (~ 50 [38]) and hundreds (~ 300 [37]), respectively (see [35] and the references cited therein). Apparently the lifetime of each PSD is long so that its eventual dissolution, which corresponds to the switching from the localized phase to nonlocalized phase (see below), is not observed, though it is *in principle* possible. We, therefore, suppose that the thermodynamic framework describing the phase change is practically applicable to our system.

As mentioned above the (quasi-)equilibrium states will be looked for in a space with four variables, $\{\sigma_R^{(z)}, \sigma_R^{(x)}, \sigma_s^{(z)}, \sigma_s^{(x)}\}$. The Landau function in our model is G (see (3)), which includes the free energies related to the interfaces between the compartments as represented in Fig. 4(a). The highest probability of realization corresponds to the maximum of $\propto e^{-G/k_B T}$, or the minimum of G , provided that the total number of membrane receptors is constrained to be constant, (Eq.2). We use a standard technique of the Lagrange multiplier (see Appendix A.1 for a brief description), which replaces the problem of constrained optimization by the following conditions, $\partial[G - \mu_R^* (A^{(z)} \sigma_R^{(z)} +$

$A^{(x)}\sigma_R^{(x)}]/\partial\sigma_R^{(\alpha)} = \partial[G - \mu_R^*(A^{(z)}\sigma_R^{(z)} + A^{(x)}\sigma_R^{(x)})]/\partial\sigma_s^{(\alpha)} = 0$, for $\alpha = z$ and x , or,

$$\frac{\partial G}{\partial\sigma_R^{(z)}} - \mu_R^*A^{(z)} = \frac{\partial G}{\partial\sigma_R^{(x)}} - \mu_R^*A^{(x)} = \frac{\partial G}{\partial\sigma_s^{(z)}} = \frac{\partial G}{\partial\sigma_s^{(x)}} = 0, \quad (10)$$

where the Lagrange multiplier μ_R^* has the meaning of the chemical potential of the membrane receptors. It is to be determined so that the constraint of Eq.2 is satisfied. These conditions, five in total including Eq.2, are sufficient to determine the five unknown variables, $\{\sigma_R^{(z)}, \sigma_R^{(x)}, \sigma_s^{(z)}, \sigma_s^{(x)}, \mu_R^*\}$. This approach was chosen because the existence of reciprocal interactions prevents a straightforward estimation of receptor number as a function of scaffold or trans-membrane signal protein number only.

Though the treatment of the model is very general and based on the principles of statistical thermodynamics, the architecture of the model is developed on the basis of the following details known about the synaptic sites: the presence of the localization signal (h_0), interactions between scaffold proteins (nonlinearity of $U_s(\sigma_s)$), especially the intermolecular attraction (i.e. the term $U_2\sigma_s^2$ with $U_2 < 0$) and interaction between scaffold proteins and receptor molecule ($\sigma_R\nu(\sigma_s)$).

IV. RESULTS: LOCALIZATION-DELOCALIZATION TRANSITION

We analyze how the local density of receptors at the synapse in the quasi-equilibrium states depends on control parameters represented by the pre-to-postsynaptic signaling (h_0) as well as the chemical potential of cytoplasmic scaffold proteins ($\mu_{s,\text{bulk}}$). One should keep in mind that, since the total synaptic and extrasynaptic number of receptors, N_R , is supposed to be constant within the time scale of our interest, the chemical potential of the receptors, μ_R^* , is not a controllable parameter (unlike that of scaffold protein, $\mu_{s,\text{bulk}}$), but is a part of the output of the quasi-equilibrium condition. This is why we did not study the variation vs μ_R^* . Eq.2 and Eq.10 can be solved numerically (see Appendix A.2 for technical details).

The values of the parameters were chosen to account for the possible experimental situations of the system. They include the proportion of membrane covered by synaptic contact, $A^{(z)}/A^{(x)}$, where we have taken $(A^{(z)}, A^{(x)}) = (0.1, 0.9)$ except for in § IV D where $(A^{(z)}, A^{(x)}) = (0.01, 0.99)$, the non-steric part of the free energy of scaffold proteins in the sub-membrane, $U_s(\sigma_s) = U_1\sigma_s + U_2\sigma_s^2 + U_4\sigma_s^4$, with $\{U_1, U_2, U_4\} = \{1, -1.15, 0.5\}$, and the factor in the scaffold protein-receptor interaction energies (see (9)), $\nu(\sigma_s) = \nu_f[1 - e^{-\nu_1(\sigma_s/\sigma_{s0}) - \nu_2(\sigma_s/\sigma_{s0})^2}]$, with $\{\nu_f, \nu_1, \nu_2\} = \{-6, 2, 1\}$. To check the robustness (see below Eq. (9)), we used $\nu(\sigma_s) = \nu_f[\nu_1(\sigma_s/\sigma_{s0}) - \tilde{\nu}_2(\sigma_s/\sigma_{s0})^2]$, with

$\{v_f, \tilde{v}_1, \tilde{v}_2\} = \{-6, 1.9, 1\}$. The units of energy and space are chosen such that $k_B T = 1$ and the saturation areal density of receptors on the membrane, σ_{R0} , and that of scaffold proteins in the sub-membrane layer, σ_{s0} , are 1 in both zones.

For a certain range of parameters, $\{h_0, \mu_{s,\text{bulk}}\}$, Eq.2 and Eq.10 have multiple solutions. When it happens, the solution chosen is the one with the minimum value of G , and therefore the maximum probability of realization, $e^{-G/k_B T}$. The phase change between different solutions corresponds to the standard criterion of the so-called Maxwell's construction, which was originally used in the Van der Waals model of vapor-liquid condensation (see below).

A. Effect of scaffold density on equilibrium

We first examine the consequences of the chemical potential of the scaffold proteins in the bulk cytoplasm, $\mu_{s,\text{bulk}}$ (Fig. 6(a)). As it varies, it modifies the densities of the receptors $\{\sigma_R^{(z)}, \sigma_R^{(x)}\}$ in the respective zones (Fig. 6(a) σ_R), and those of the scaffold proteins $\{\sigma_s^{(z)}, \sigma_s^{(x)}\}$ in the sub-membrane layer (Fig. 6(a) σ_s). The chemical potential $\mu_{s,\text{bulk}}$ cannot be defined as an absolute number, but its variation contains the meaning: the higher its value, the more concentrated the scaffold proteins in the bulk layer.

As seen on the curve, there is a region of $\mu_{s,\text{bulk}}$ values where three solutions can be found with corresponding values of G . Among these, the one corresponding to the equilibrium was determined as that where G has the minimum value for a given $\mu_{s,\text{bulk}}$, or a given density of cytoplasmic scaffold protein. The selected solutions are shown by solid curves in the figures. For completeness, Maxwell's construction is briefly summarized in the rest of this subsection. When following a curve for the density $\sigma_R^{(z)}$ (e.g. on Fig. 6(a) σ_R) from the minimum value of $\mu_{s,\text{bulk}}$ (left-end) to the maximum (right-end), there is a portion where $\mu_{s,\text{bulk}}$ decreases. This phenomenon occurs simultaneously for all the density variables, $\sigma_R^{(z)}$ and $\sigma_R^{(x)}$ in Fig. 6(a) σ_R , $\sigma_s^{(z)}$ and $\sigma_s^{(x)}$ in Fig. 6(a) σ_s . It applies also to the curve of G (Fig. 6(a) G). The portion of the curve where $\mu_{s,\text{bulk}}$ decreases corresponds to the branch where the value of G is maximum among the three points corresponding to the *same* value of $\mu_{s,\text{bulk}}$. The maximum in G implies the minimum in the probability of realization $\propto e^{-G/k_B T}$. The portion of the curve where the value of $\mu_{s,\text{bulk}}$ decreases thus corresponds neither to an equilibrium nor to a metastable equilibrium. So we exclude this portion of the curves of Fig. 6(a) σ_R and Fig. 6(a) σ_s .

The crossing point in Fig. 6(a) G indicates the situation where two equilibria can occur with the

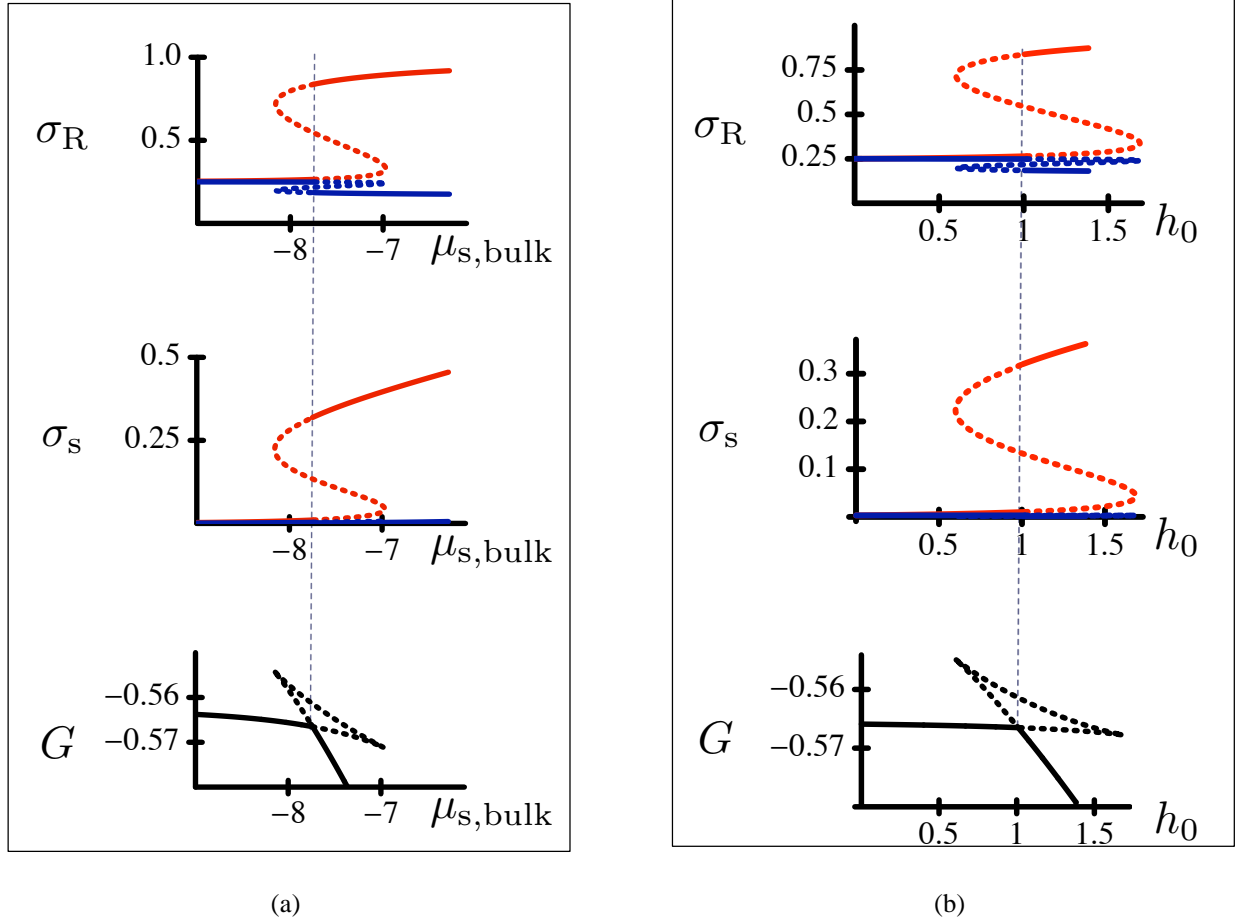


FIG. 6: (Color online) (a) Transition (switching) induced by the chemical potential of the scaffold protein in the bulk cytoplasm, $\mu_{s,bulk}$ (horizontal axis). (The value of h_0 is fixed at $h_0 = 1$.) *Top* (σ_R): Densities of the membrane receptors in the membrane layer. *Middle* (σ_s): Densities of the scaffold proteins in the sub-membrane layer. The red [blue] curves represent, respectively, the densities in the synaptic [extrasynaptic] zones. *Bottom* (G): Free energy of the system. The vertical dashed line passing through the figures marks the point of phase change, to switch the branch of solutions. Those parts represented by dashed curves are not realizable as quasi-equilibrium.

(b) Switching induced by the trans-membrane signal, h_0 . (The value of $\mu_{s,bulk}$ is fixed at $\mu_{s,bulk} = -7.747$.)

same probability. The solution branches are to be switched at this crossing point. The equilibrium densities corresponding to this point can be identified in Fig. 6(a) σ_R and Fig. 6(a) σ_s . The switching indicates a discontinuous transition of mode of the partitioning receptors and scaffold proteins between extrasynaptic and synaptic zones. This redistribution is a *phase change* in the sense that we discussed in § III C. The situation is schematically shown in Fig. 7(a). In one phase, which we call the *nonlocalized phase*, the receptors are found at almost the same density in synaptic

and extrasynaptic zones, while there is no accumulation of scaffold proteins. In the other phase, which we call the *localized phase*, receptors accumulate abundantly in the synaptic zone, and are diluted in the extrasynaptic zone. And the scaffold proteins also accumulate in the synaptic zone. This dramatic contrast in density is genuinely collective in the sense that we have carefully chosen the parameters of the model so that no phase change takes place without reciprocal coupling between the receptors and scaffold proteins, $g_{\text{mem-sub}}^{(\alpha)}$. That is, despite the attractive interaction among the scaffold proteins, $U_s(\sigma_s)$, promoting the accumulation of the scaffold proteins, and the trans-membrane signal, $(-h_0)$, favoring their density in the synaptic zone, they are not enough to realize the distinct accumulation of molecules at the synaptic zone if $g_{\text{mem-sub}}^{(\alpha)} \equiv 0$. In other words, the accumulation would not occur if there were no receptors on the membrane.

B. Effect of trans-membrane signal on equilibrium

The trans-membrane signal imposed by the presynaptic element specifies the organization of the postsynaptic plasma membrane. This determines the locus where receptors are to accumulate, and is likely to induce an initial metastable state for the formation of the synapse. In this second study, we therefore analyze the effect of the amount of this trans-membrane signal, h_0 . Fig. 6(b) shows the densities of the receptors in the respective zones, similar to Fig. 6(a) when changing h_0 . Again, by monitoring the values of G , the phase change is identified as the self-crossing point of G . Because of the collective effect, a continuous (quasi-equilibrium) increase of the signal h_0 induces a sudden accumulation of the molecules in the synaptic zone.

C. Phase diagram

The notion that scaffold and adhesion molecules act cooperatively in the formation of the postsynaptic density is emphasized in Fig. 7(a). When we allow both the parameters $\mu_{s,\text{bulk}}$ and h_0 to vary, our main results are summarized in the form of a phase diagram on the plane of $(\mu_{s,\text{bulk}}, h_0)$, see Fig. 7(b). This diagram was numerically determined using the technique described in Appendix A.2. We observe that the nonlocalized and localized phases are separated by a rather straight boundary. The reason for this almost straight phase boundary has to be found in the phenomenon of the localization itself. Two requirements are to be satisfied. 1) in the localized phase the term $(\mu_{s,\text{bulk}} + h_0)\sigma_s^{(z)}$ in the free energy G is important while $\mu_{s,\text{bulk}}\sigma_s^{(x)}$ is negligible; (because

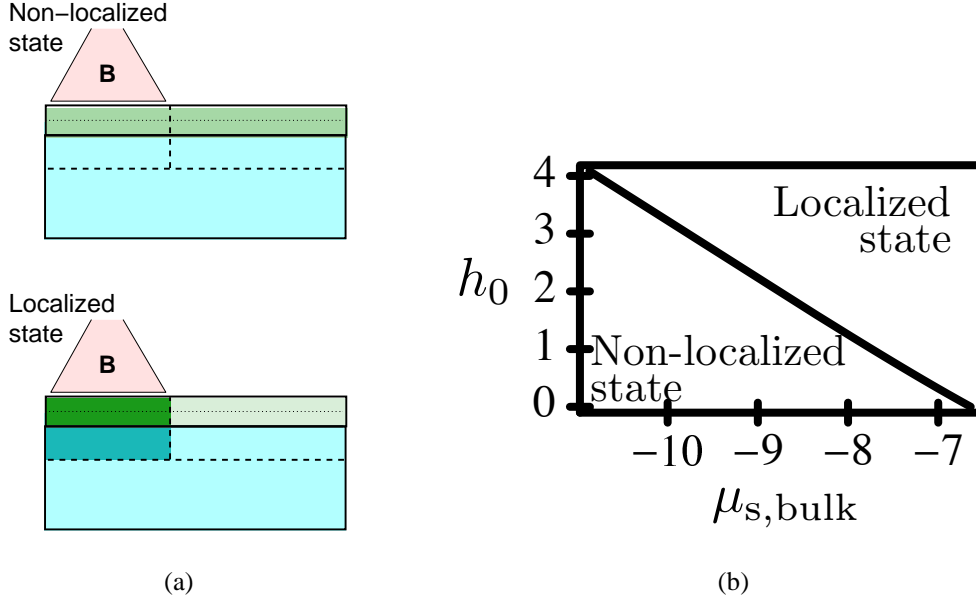


FIG. 7: (a) (Color online) Densities of receptors (in green) and scaffold proteins (in cyan) in the nonlocalized state (top) and localized state (bottom) are shown schematically by concentration of the colors.

(b) Phase diagram of localized *vs* nonlocalized phases on the plane of the controlling parameters. The almost straight diagonal curve is the numerical result.

$\sigma_s^{(x)} \ll \sigma_s^{(z)}$), and 2) in the delocalized phase the signal h_0 is not important (because $\sigma_s^{(z)}$ is small). Therefore, the sum $(\mu_{s,bulk} + h_0)$ is the term that effectively influences the quasi-equilibrium phase.

D. Non-relevant depletion of extrasynaptic receptors upon localization transition

As illustrated in Figs. 6(a) and 6(b), the receptor density at the synapses, $\sigma_R^{(z)}$, can be localized at the expense of its decrease outside synapse, $\sigma_R^{(x)}$, when the synapses occupy 10 percent of the surface, $(A^{(z)}, A^{(x)}) = (10\%, 90\%)$. It is, therefore, of interest to check if the localization transition can take place if $A^{(z)}$ is much smaller than $A^{(x)}$, e.g. $(A^{(z)}, A^{(x)}) = (1\%, 99\%)$, in the following two lines of reasonings: firstly, the presence of the transition confirms that the decrease in the extrasynaptic receptor density $\sigma_R^{(x)}$ is not necessary for the localization transition, though it may rather be a inhibitory factor; secondly, the localization transition with a small synaptic area, like 1% of the total membrane, may qualitatively simulate the initial stage of synaptogenesis. We have verified numerically that the localization of both the receptors and the scaffold proteins occurs even with the area fractions, $(A^{(z)}, A^{(x)}) = (1\%, 99\%)$. The densities $\sigma_R^{(z)}$ and $\sigma_s^{(z)}$ show a similar

jump as in Figs. 6(a) or 6(b) while $\sigma_R^{(x)}$ and $\sigma_s^{(x)}$ for the extrasynaptic zone display minute change at the localization transition (data not shown). With such a small fraction of synaptic area the conservation of the total number of receptors, Eq.2, is effectively not a constraining factor, and the persistence of the localization transition indicates that the mechanism of the localization transition remains in *local* exchanges of molecules between a synaptic site and its environment.

E. Effect of weakening of the receptor-scaffold protein interaction

The interaction between the receptors and the scaffold proteins can be modified by phosphorylation [39]. In our model, the weakening or strengthening of molecular interactions has effects on the quasi-equilibrium state of PSD. It can be simulated by modifying the profile of the function $v(\sigma_s^{(\alpha)}) = v_f [1 - e^{-v_1 \left(\frac{\sigma_s}{\sigma_{s0}}\right) - v_2 \left(\frac{\sigma_s}{\sigma_{s0}}\right)^2}]$. To this aim, we varied the global factor, v_f , which accounts for the saturating binding strength. We found (data not shown) (i) that when v_f is reduced to 70% of the original value (-6.0 in the units of our model), the localization transition *vs* $\mu_{s,bulk}$ almost disappears, while the receptor density in the synapse, $\sigma_s^{(z)}$, has strong non-linear behavior; (ii) furthermore, when v_f is reduced to 50% of the original value, there is no more localization transition and $\sigma_s^{(z)}$ displays a smooth sigmoidal dependence on $\mu_{s,bulk}$.

F. Limit of robust characters

The stability of receptor density in the synaptic region $\sigma_R^{(z)}$ is an indication of the robustness of the localized state. This robustness, however, has a limit. The quasi-equilibrium state for different (conserved) values of the total receptor number, N_R (between 0.02 and 0.4 in the arbitrary unit) was estimated with fixed values of h_0 and $\mu_{s,bulk}$. In the localized state the receptor density in the synaptic region, $\sigma_R^{(z)}$ (as well as $\sigma_s^{(z)}$), is almost saturated and constant while that in the extrasynaptic region increases roughly proportionally to N_R . But if N_R is less than a critical value, $N_R^{(loc)} \simeq 0.16$, then the localized state is destroyed and the receptor densities in synaptic and extrasynaptic regions are almost the same and proportional to N_R . Therefore, the robustness is closely related to the cooperative effect. That the localization disappears for too small value of v_f (§ IV E) implies that the robustness is also closely related to the reciprocal stabilization of the PSD.

V. DISCUSSION

A. Summary of the results and comparison with other theories

In this paper we present a minimal three-layer two-compartment model to describe the formation of the postsynaptic assembly of membrane receptors and scaffold proteins. We found the discontinuous phase change between the nonlocalized and localized phases. In the localized phase, the stable high density of receptors at synaptic sites is compatible with the mobility of individual receptors. This accounts for the observation that synapse formation is almost an all-or-none process, operating on a short time scale in the range of the diffusion constant of individual molecules. (Here one should take into account not only the diffusion of receptors but also the local turnover of scaffold proteins.) We note that the *latency time* for synapse formation should be distinguished from the *duration of synapse formation*, which we discuss here. The former time results from the metastability of the receptor-scaffold assembly. This is indeed one of the main message of this paper (see V.B *b* and *c* below). Although our model assumes the quasistatic equilibrium, such decoupling between kinetics and thermodynamics (§ II B) should also be true even if the system is slightly out of equilibrium. Such flexibility is the basis of the responsiveness of the synaptic junction (see, for example, a review [40]). Understanding how the number of receptors is determined at steady state as a set-point of dynamic equilibrium provides the mechanism by which this number can be modified during plastic changes of synaptic strength (the gain of information transfer).

Recently, a new model has been proposed [41] in which the stability of receptor density is compatible with individual receptor turnover. This model deals only with the membrane receptor zone in the synaptic compartment as we defined it. Nevertheless, it accounts for the key idea of cooperativity in maintaining the stable density of receptors, as too does our model. However it does not take into account the interaction of receptors with scaffolding molecules nor the chemical potentials resulting from concentration differences in the cellular compartments. Therefore, the model we propose complements the concept of cooperativity within a more realistic framework based on experimental knowledge demonstrating the exchanges between extrasynaptic and synaptic receptors [9]. This concept of cooperativity has been suggested to operate between the acetylcholine receptor and the 43kD/rapsyn protein [42]. Recently, Fusi *et al.* proposed a cascade mechanism to generate different time scales of synaptically stored memories [43], which sheds light on the quasi-equilibrium approach that we propose. As the kinetics are independent of the

stability of postsynaptic molecular construction, different time scales can coexist to account for the dynamic turnover of constituent molecules in the postsynaptic density. The layered structure of the postsynaptic multi molecular assembly reflects a cascade of interactions (the trans synaptic molecule signaling to the scaffold protein assembly and then receptor accumulation via reciprocal stabilization with the scaffold proteins).

B. Implications of the results and qualitative comparison with experiments

a. Collective stabilization justifies the non-stoichiometry. Only 20 to 30% of PSD-95, a scaffold protein present at excitatory synapses, in the sub-membrane layer is likely to be bound to receptors at steady state [37, 38]. This proportion, well below 100%, is accounted for by our model. Since the ratios $\sigma_R^{(z)}/\sigma_s^{(z)}$ and $\sigma_R^{(x)}/\sigma_s^{(x)}$ are determined by the reciprocal and collective stabilization, there is no reason for them to be a rational number. From the values of the densities of receptors ($\sigma_R^{(z)}, \sigma_R^{(x)}$) and of scaffold proteins ($\sigma_s^{(z)}, \sigma_s^{(x)}$) (in Fig.6(a) and (b)), we can read out the proportion of receptors interacting with scaffold proteins, i.e. $\sigma_R^{(z)}/\sigma_s^{(z)}$ or $\sigma_R^{(x)}/\sigma_s^{(x)}$ in units of σ_{R0}/σ_{s0} (data not shown). In the synaptic zone, the ratio $\sigma_R^{(z)}/\sigma_s^{(z)}$ increases dramatically upon the localization transition, while in the extrasynaptic zone the ratio $\sigma_R^{(x)}/\sigma_s^{(x)}$ decreases only slightly upon the localization. This is due to differences in surface area [37, 38].

b. Competitive binding can destroy the localized phase. Disturbing molecules (such as ones producing dominant-negative competitive binding) modifies the energy profiles by altering the chemical potential $\mu_{s,\text{bulk}}$. In Appendix.B the equilibrium theory of competitive binding is summarized briefly. The theory shows that the competitive molecule species (e.g. B) versus the principal species (e.g. A) effectively reduces the chemical potential of the latter, μ_A^0 by a quantity $\Delta\mu_A^0 = -k_B T \ln[1 + e^{(U_B + \mu_B^0)/k_B T}]$, where U_B and μ_B^0 are the binding energy and the external chemical potential, respectively, for the competitive/dominant-negative molecule. As we found that the low chemical potential $\mu_{s,\text{bulk}}$ destabilizes the localized phase, we predict that the competitive binding with scaffold proteins tends to destabilize the localized phase.

c. The fate of PSD after sudden disappearance of localization signal should depend nonlinearly on the cytoplasmic scaffold protein concentration. Although our approach is quasistatic, we can draw some conclusions about the non-quasistatic phenomena since the response of the postsynaptic density (PSD) to a sudden disappearance of the localization signal, h_0 , should depend on the other parameters of the system (see [44] for synapses during development and [45, 46] for

mature synapses). As seen on the phase diagram, Fig.7:(b), the localization transition occurs even when $h_0 = 0$ if the concentration of the scaffold protein is large enough (or, $\mu_{s,bulk} \geq -6.3$ in Fig.7:(b)). For $\mu_{s,bulk}$ near this threshold value, the sudden disappearance of h_0 will leave, at least transiently, the PSD as a (meta)stable state for $h_0 = 0$. However, if $\mu_{s,bulk}$ was far below the threshold value, then the aggregate will be disrupted rapidly by lateral diffusion after the disappearance of h_0 . In conclusion we predict that the life-time of the PSD after the sudden disappearance of h_0 depends on $\mu_{s,bulk}$ in a highly non-linear manner. The detailed dynamic response, however, is beyond the scope of the present quasi-equilibrium framework of our paper.

d. Delayed time for the construction of a new synapse can be due to the metastable nonlocalized phase. A complementary issue to the above paragraph is “how long would a new synapse take to assemble?” Experimentally, the assembly of a new PSD takes at least tens of minutes, more likely 1-2 hours [47], which is not rapid, given the characteristic diffusion constant of individual receptors (in the order of $10^{-2}\mu\text{m}^2/\text{sec}$). This time lag supports our model of cooperative interaction underlying synaptic localization of receptors. When the expression of the scaffold proteins in the cytoplasm raises $\mu_{s,bulk}$ just up to the localization transition point, the nonlocalized state remains still metastable. Under such conditions the clustering of PSD must wait for the random rare event (“nucleation”) which assembles a critical concentration of receptors as well as scaffold proteins. We then predict that the waiting time of the nucleation should be stochastically distributed, typically obeying an exponential distribution.

e. The model accounts for the triggering role of trans-membrane signal on the localization. The phenomenon of localization could be intuitively postulated from the known molecular interactions, for example, between neuroligin and the scaffold protein PSD-95 [48]. Experimental data indicate that the neurexin-neuroligin heterophilic interaction induces the formation of the postsynaptic micro-domain [48], and that, once it begins, it is a rapid phenomenon, taking place within minutes [49]. The present model is consistent with these observations. That is, the formation of postsynaptic micro-domains is almost an all-or-none phenomenon involving a phase change, and is imposed by the presynaptic contact.

f. The model admits the spontaneous formation of sub-membrane aggregates. In the early period of synaptogenesis spontaneous formation of sub-membrane aggregates of scaffold proteins have been observed, notably at the locations of dendrite-dendrite contact or dendrite-substrate contact[50, 51]. In our model, spontaneous localization of scaffold proteins can be realized without receptors or without the transsynaptic bias, h_0 , if we modify the parameter characterizing the

attractive interaction among scaffold proteins, that is, $|U_2|$ in $U_s(\sigma_s)$ (see (5)).

C. Future problems

As future problems we should incorporate other factors that might exert influence on synaptic receptor clustering. In particular, we may take into account the mechanism involving aggregation of receptors through direct interaction with an extracellular-matrix molecule [52], the activation of receptors which is indirectly related to the electrodiffusion of charged neurotransmitter molecules [53], and the dendritic spine geometry (volume of spine head and spine length), which is strongly correlated with the number of receptors on the spine [54].

An important question is how much time an individual receptor spends in the synaptic zone. At steady state, the fraction of time spent by a particular receptor on a particular synaptic contact should be proportional to the density of the receptors at the contact. This is true if all receptors are well mixed so that there is no separation between the permanently immobile receptors and mobile receptors. Experimentally, single-particle tracking measurements have established that about half of the receptors are mobile at central excitatory synapses [20]. In contrast, FRAP experiments of glutamate receptors at *Drosophila* neuromuscular junctions suggest that they are immobilized once they enter into the postsynaptic domain [55]. Models to assess these observations must go beyond the simple dichotomy of synaptic - vs extrasynaptic - zones.

A major unsolved problem is the determining mechanism of the postsynaptic micro-domain. The size of this domain, although variable, is maintained in a relatively narrow range, 100-300 nm in diameter [56]. In double transfection experiments with glycine receptor and its associated scaffold proteins, it was found that the aggregates of scaffold proteins had a size close to that of postsynaptic micro-domains [57] even in the absence of presynaptic terminals. However, this will not specify the size of the localized cluster of scaffold proteins. One may conjecture several different mechanisms for the regulation of the size of postsynaptic micro-domains. A cost of curvature driven energy of a microdomain structure might define an optimal size of aggregates as found for clathrin-coated vesicle formation[58]. Or, the steric repulsion among molecules reflecting their three-dimensional arrangement may limit the size of the cluster [32].

Acknowledgments

We acknowledge Jean-François Joanny for reading the original manuscript and providing a few references. We also acknowledge a referee for bringing numerous recent references to our attention. This work was supported by a grant from the Agence Nationale de la Recherche, ANR 05-Neur-043-02.

Appendix A. Technical notes

A.1 Brief summary of the Lagrange multiplier method

This method finds stationary points (local maxima etc.) of $f(\mathbf{x})$ with the constraint $g(\mathbf{x}) = 0$, where $\mathbf{x} = (x_1, \dots, x_n) \equiv \{x_i\}$. A point of stationary point, \mathbf{x}^* , together with a constant called the Lagrange multiplier, λ , must satisfy the following condition:

$$g(\mathbf{x}^*) = 0, \quad \left. \frac{\partial(f - \lambda g)}{\partial x_i} \right|_{\mathbf{x}=\mathbf{x}^*} = 0, \quad i = 1, \dots, n. \quad (11)$$

The reason is that at \mathbf{x}^* the contour surface of $f(\mathbf{x}) = f(\mathbf{x}^*)$ and that of $g(\mathbf{x}) = 0$ must share the same tangential plane, and that, for any function, say $\phi(\mathbf{x})$, the normal vector of a tangential plane is along $(\partial\phi/\partial x_1, \dots, \partial\phi/\partial x_n)$, which can be easily verified in the case of a line $ax_1 + bx_2 = c$.

A.2 Numerical solution procedure

Formally, the problem is to solve n coupled non-linear equations for $(n + 1)$ variables, $f_i(x_1, \dots, x_n, x_{n+1}) = 0$ ($i = 1, \dots, n$). Once we have a particular solution $(x_1, \dots, x_n, x_{n+1})$, then we may use the differential equations describing the solution curve in the space of $\mathbf{x} \equiv (x_1, \dots, x_n, x_{n+1})$: $\sum_{j=1}^{n+1} M_{ij} d\mathbf{x}_j = 0$ ($i = 1, \dots, n$), where M is the $n \times (n + 1)$ matrix containing the components, $M_{ij} \equiv \partial f_i / \partial x_j$ ($i = 1, \dots, n$ and $j = 1, \dots, n + 1$). The latter equations can be solved using the cofactor of M , which we denote by \tilde{M} (i.e., $\tilde{M}_{i,j}$ is $(-1)^{i+j}$ times the minor entry of $M_{i,j}$):

$$\frac{d\mathbf{x}}{ds} = (\tilde{M}_{n+1,1}, \dots, \tilde{M}_{n+1,n+1})^t, \quad (12)$$

where s is a parameter along the solution curve.

In the context of solving Eq.2 and Eq.10 we have $n = 5$. The variable is $\mathbf{x} = (\sigma_R^{(z)}, \sigma_R^{(x)}, \sigma_s^{(z)}, \sigma_s^{(x)}, \mu_R^*, \xi)$, where the sixth component ξ stands for either the parameter $\mu_{s,\text{bulk}}$ (§ IV A) or h_0 (§ IV B). To find the phase boundary (§ V, Fig. 7(b)), we have $n = 11$, i.e. twice the five conditions of Eq.2 and Eq.10 for each phase, plus the equality of the total free energy, G . The variables \mathbf{x} consists of twice the five variables, $\{\sigma_R^{(z)}, \sigma_R^{(x)}, \sigma_s^{(z)}, \sigma_s^{(x)}, \mu_R^*\}$, for the coexisting phases, plus $\mu_{s,\text{bulk}}$ and h_0 .

Appendix B: Effect of competitive binding

We take as the Helmholtz free energy $F/k_B T = -n_A \frac{U_A}{k_B T} - n_B \frac{U_B}{k_B T} + n_A \ln(n_A/n) + n_B \ln(n_B/n) + n_V \ln(n_V/n)$, where n_A and n_B are the number of the A [B] molecules occupying among the n binding sites, respectively, and $n_V = n - n_A - n_B$. We impose the chemical equilibrium conditions with the solvent chemical potentials for A and B, which we denote by μ_A^0 and μ_B^0 , respectively; $\mu_A^0 = \partial F / \partial n_A$ and $\mu_B^0 = \partial F / \partial n_B$. In the absence of B molecules (i.e. $\mu_B^0 = -\infty$), equilibrium condition for the A molecule binding writes $\mu_A^0 = -U_A + k_B T \ln[n_A / (n - n_A)]$, while for finite μ_B^0 , the right hand side of this condition is shifted by $-\Delta\mu_A^0 (> 0)$, where $\Delta\mu_A^0 \equiv -k_B T \ln[1 + e^{(U_B + \mu_B^0) / k_B T}]$. This implies that the attractive energy $-U_A$ for A molecule is partly cancelled by this amount due to the competitive/dominant-negative molecules, B. If $U_B \ll k_B T$, the effect is small, in the order $k_B T$ (more precisely $\simeq -k_B T e^{(U_B + \mu_B^0) / k_B T}$). Contrastingly, large $U_B / k_B T$ has a strong influence of the competing molecules due to the interference, $\Delta\mu_A^0 \simeq -(U_B + \mu_B^0)$.

Appendix C. Note for the biologists

In this appendix we explain in general terms, easily understandable for biologists, the object of the modelling accounting for the compatibility between synaptic stability and molecular mobility.

The stability of the synaptic structure, with its mobile receptors, is a complex matter, because the local turnover (at synapses) of the constituent elements is shorter than the lifetime of the synapse (see comment by [59]). In the light of the dynamics of individual molecules such as diffusion in the plane of the plasma membrane for receptors and of spatial 3D diffusion of scaffolding molecules in the cytosol, it was necessary to establish a theoretical background accounting for the accumulation of receptors at synapses. The present model has been developed including the extrasynaptic membrane.

It stresses the *quasi-equilibrium* which is valid on a time scale shorter than that of receptor turnover on the membrane. It is not known if the turnover by exocytosis and endocytosis promotes exchange of receptors between the synaptic and extrasynaptic zones, or whether such active exchange has a role on large time scales. However, this raises the question of multi molecular assembly as a global entity in which regulation can operate without destroying the integrity of the structure. In more biological terms, the important question is how molecules such as receptors or scaffold proteins can be added or removed while maintaining the synaptic function with variable gain. The present model provides a general framework in which it is now possible to conceive of molecular interactions in terms of chemical potentials and, therefore, to model a kinetic view of the synaptic multi-molecular assembly. It is also expected that the model we propose will allow a unification of the different levels of postsynaptic events, from the chemical interaction between receptors and scaffolding molecules up to the plasticity of synaptic transmission. In this context we mention three aspects which may help refine our study in the future: heterogeneity of time scales, collective stabilization, adaptation and molecular exploration upon PSD formation.

The components used for the modelling are of the same nature as those used in physical chemistry to account for the thermodynamics of chemical reactions, which also holds in living system. The model predicts a discontinuous increase of the density of receptors at the synaptic contact through the transition to the localization regime. Unless there is an unusual kinetic mechanism to increase the mobility of individual receptors during the localization transition, the increase of receptor density in a synaptic zone should also imply a lengthening of the residence time of individual receptors. However, one should stress that the stabilization of receptor density (number of receptors) in the synaptic zone with indefinite lifetime is compatible with a finite residence time of an individual receptor on a synaptic site. Thus, the persistence of the individual mobility of receptors facilitates fast adaptation of receptor numbers in relation to changes in neuronal activity.

Another concept which arises from the present model is the notion that stabilization is a *reciprocal mechanism*. In other terms, scaffold proteins stabilize receptors, and receptors stabilize scaffold proteins. This means that the local turnover of a given protein is not likely by itself to determine the turnover of the structure. In the context of synaptogenesis, reciprocity ensures the synchronized and adaptive construction of the synapses, since neither receptor nor scaffold protein nor transsynaptic interaction alone can stabilize the localization. Reciprocity introduces robustness against the fluctuations in total receptor number associated with exo-/endocytosis at extrasynaptic sites. In addition, the reciprocity is likely to attenuate the amplitude of stochastic fluctuations of

the receptor numbers at each synaptic site.

Another major outcome of the proposed model is that it accounts for changes during synaptic plasticity or even during synapse formation, which may result from changes in receptor number in the plasma membrane and/or from changes in the density of scaffold proteins in the cytosol. It explains how changes in densities, i.e. chemical potentials, of receptors and scaffold proteins lead to a new steady state of the postsynaptic molecular assembly: the *cooperativity* underlying the discontinuous change in density distributions allows the system to switch from one point of equilibrium (set-point) to another one, by small changes in key parameters (trans-synaptic signal, cytoplasmic density of scaffold proteins, density of extrasynaptic receptor). At the molecular level, the mechanisms for the stoichiometry of interaction of receptors with individual scaffold proteins are not fully understood.

The model is consistent with the fact that, once the formation of synaptic contacts starts, it is likely to be a rapid process as the system is cooperative and almost auto-catalytic. That the recruitment kinetics of various PSD molecules are remarkably similar indicates that PSD assembly rate is governed by a common upstream rate-limiting process [60]. In this context it has been observed that the receptor and scaffold proteins can be already associated on the extrasynaptic membrane [61]. Intracellular packages of NMDA receptors (NMDA-R) or AMPA receptors (AMPA-R) with the scaffold protein PSD-95 have been identified [62, 63]. Also packages of glycine receptor (Gly-R) and its scaffold protein partner, gephyrin, were found to be transported through the secretion pathway from the Golgi apparatus to the membrane [64]. Therefore two mechanisms are cooperative for the assembly of a new PSD: firstly, as mentioned above, pre-assembly of receptor-scaffold complexes in the secretion pathway [65], secondly, the high diffusion rate of the receptors, which makes them explore large areas of plasma membrane ([66] and the references cited therein). Therefore, molecules at any location of the cell surface may encounter with a high frequency. As a consequence, a local trans-synaptic interaction creates a potential well that will rapidly trap the diffusing molecules. These chemical kinetics have to be reconciled with specific biological mechanisms. This can now be achieved because the behavior of individual molecules can be monitored (see [66]), therefore allowing access to mechanisms normally hidden in the convoluted statistics of the behavior of large numbers of molecules.

[1] R. Malinow and R. C. Malenka, *Annu. Rev. Neurosci.* **25**, 103 (2002).

- [2] M. Sheng and M. J. Kim, *Science* **298**, 776 (2002).
- [3] D. S. Bredt and R. A. Nicoll, *Neuron* **40**, 361 (2003).
- [4] A. Verkhovskiy, T. Svitkina, and G. Borisy, *Current Biol.* **9**, 11 (1999).
- [5] B. Alberts, A. Johnson, J. Lewis, M. Raff, K. Roberts, and P. Walter, *Molecular Biology of the Cell* (Garland Science (New York), 2002), 4th ed.
- [6] K. Sekimoto, J. Prost, F. Jülicher, H. Boukellal, and A. Bernheim-Grosswasser, *Eur. Phys. J. E* **13**, 247 (2004).
- [7] K. Kruse, J.-F. Joanny, F. Jülicher, J. Prost, and K. Sekimoto, *Phys. Rev. Lett.* **92**, 078101 (2004).
- [8] K. Kruse, J.-F. Joanny, F. Jülicher, J. Prost, and K. Sekimoto, *Eur. Phys. J. E* **16**, 5 (2005).
- [9] A. Triller and D. Choquet, *Trends Neurosci.* **28**, 133 (2005).
- [10] S. J. Moss and T. Smart, *Nat. Rev. Neurosci.* **2**, 240 (2001).
- [11] M. Sheng and C. Sala, *Annu. Rev. Neurosci.* **24**, 1 (2001).
- [12] D. S. Faber, P. G. Funch, and H. Korn, *Proc. Natl. Acad. Sci. U. S. A.* **82**, 3504 (1985).
- [13] D. M. Kullmann and F. Asztely, *Trends Neurosci.* **21**, 8 (1998).
- [14] B. A. Clark and S. G. Cull-Candy, *J. Neurosci.* **22**, 4428 (2002).
- [15] A. Momiyama, R. A. Silver, M. Häusser, T. Notomi, Y. Wu, R. Shigemoto, and S. G. Cull-Candy, *J. Physiol.* **549**, 75 (2003).
- [16] A. Scimemi, A. Fine, D. M. Kullmann, and D. A. Rusakov, *J. Neurosci.* **24**, 4767 (2004).
- [17] E. A. Newman, *Trends Neurosci.* **26**, 536 (2003).
- [18] B. Chih, H. Engelman, and P. Scheiffele, *Science* **307**, 1324 (2005).
- [19] N. K. Hussain and M. Sheng, *Science* **307**, 1207 (2005).
- [20] D. Choquet and A. Triller, *Nat. Rev. Neurosci.* **4**, 251 (2003).
- [21] L. D. Landau and E. M. Lifshitz, *Statistical Physics : Part 1 (Course of Theoretical Physics, Volume 5)* (Butterworth-Heinemann, 1998), 3rd ed.
- [22] D. W. Allison, A. S. Chervin, V. I. Gelfand, and A. M. Craig, *J. Neurosci.* **20**, 4545 (2000).
- [23] D. van Effenterre and D. Roux, *Europhys. Lett.* **64**, 543 (2003).
- [24] A. S. Smith and U. Seifert, *Phys. Rev. E* **71**, 061902 (2005).
- [25] S. Sarda, D. Pointu, F. Pincet, and N. Henry, *Biophys. J.* **86**, 3291 (2004).
- [26] D. Andelman and J. F. Joanny, *J. Phys. II France* **3**, 121 (1993).
- [27] V. A. Derkach, M. C. Oh, E. S. Guire, and T. R. Soderling, *Nat. Rev. Neurosci.* **8**, 101 (2007).
- [28] H. Rasmussen, T. Rasmussen, A. Triller, and C. Vannier, *Mol. Cell Neurosci.* **19**, 201 (2002).

- [29] S. Okabe, T. Urushido, D. Konno, H. Okado, and K. Sobue, *J. Neurosci* **21**, 9561 (2001).
- [30] T. Nakagawa, J. A. Engler, and M. Sheng, *Neuropharmacology* **47**, 734 (2004).
- [31] E. N. Star, D. J. Kwiatkowski, and V. N. Murthy, *Nat. Neurosci.* **5**, 239 (2002).
- [32] J. J. Sieber, K. I. Willig, C. Kutzner, C. Gerding-Reimers, B. Harke, G. Donnert, B. Rammner, C. Eggeling, S. W. Hell, H. Grubmüller, et al., *Science* **317**, 1072 (2007).
- [33] C. Bedet, J. C. Bruusgaard, S. Vergo, L. Groth-Pedersen, S. Eimer, A. Triller, and C. Vannier, *J. Biol. Chem.* **281**, 30046 (2006).
- [34] J. M. Fritschy, R. J. Harvey, and G. Schwarze, *Trends Neurosci.* **31**, 257 (2008).
- [35] M. Sheng and C. C. Hoogenraad, *Annu. Rev. Biochem.* **76**, 1 (2006).
- [36] M. Masugi-Tokita, E. Tarusawa, M. Watanabe, E. Molnár, K. Fujimoto, and R. Shigemoto, *J. Neurosci.* **27**, 2135 (2007).
- [37] X. Chen, L. Vinade, R. D. Leapman, J. D. Petersen, T. Nakagawa, T. M. Phillips, M. Sheng, and T. S. Reese, *Proc. Natl. Acad. Sci. U. S. A.* **102**, 11551 (2005).
- [38] M. B. Kennedy, *Science* **290**, 750 (2000).
- [39] M. M. Zita, I. Marchionni, E. Bottos, M. Righi, G. D. Sal, E. Cherubini, and P. Zacchi, *EMBO J.* **26**, 1761 (2007).
- [40] T. Misteli, *J. Cell. Biol.* **155**, 181 (2001).
- [41] H. Z. Shouval, *Proc. Natl. Acad. Sci. U. S. A.* **102**, 14440 (2005).
- [42] E. Yeramian and J.-P. Changeux, *C. R. Acad. Sci. III* **302**, 609 (1986).
- [43] S. Fusi, P. J. Drew, and L. Abbott, *Neuron* **45**, 599 (2005).
- [44] A. J. Smolen, *Brain Res.* **227**, 49 (1981).
- [45] T. Gentshev and C. Sotelo, *Brain Res.* **62**, 37 (1973).
- [46] T. Seitanidou, M. A. Nicola, A. Triller, and H. Korn, *J. Neurosci.* **12**, 116 (1992).
- [47] H. V. Friedman, T. Bresler, C. C. Garner, and N. E. Ziv, *Neuron* **27**, 57 (2000).
- [48] P. Scheiffele, *Annu. Rev. Neurosci.* **26**, 485 (2003).
- [49] T. A. Basarsky, V. Parpura, and P. G. Haydon, *J. Neurosci.* **14**, 6402 (1994).
- [50] I. Colin, P. Rostaing, and A. Triller, *J. Comp. Neurol.* **374**, 467 (1996).
- [51] I. Colin, P. Rostaing, A. Augustin, and A. Triller, *J. Comp. Neurol.* **398**, 359 (1998).
- [52] A. Dityatev and M. Schachner, *Nat. Rev. Neurosci.* **4**, 456 (2003).
- [53] S. Sylantsev, L. P. Savtchenko, Y. Niu, A. I. Ivanov, T. P. Jensen, D. M. Kullmann, M.-Y. Xiao, and D. A. Rusakov, *Science* **319**, 1845 (2008).

- [54] M. Matsuzaki, G. C. Ellis-Davies, T. Nemoto, Y. Miyashita, M. Iino, and H. Kasai, *Nat. Neurosci.* **4**, 1086 (2001).
- [55] T. M. Rasse, W. Fouquet, A. Schmid, R. J. Kittel, S. Mertel, C. B. Sigrist, M. Schmidt, A. Guzman, C. Merino, G. Qin, et al., *Nat. Neurosci.* **8**, 898 (2005).
- [56] A. Peters, S. L. Palay, and H. deF. Webster, *Fine Structure of the Nervous System. Neurons and their Supporting Cells* (Oxford University Press, U.S.A., 1991), 3rd ed.
- [57] J. Meier, C. Meunier-Durmort, C. Forest, A. Triller, and C. Vannier, *J. Cell. Sci.* **113**, 2783 (2000).
- [58] A. Gilbert, J. P. Paccaud, and J. L. Carpentier, *J. Cell. Sci.* **110**, 3105 (1997).
- [59] M. Sheng and T. Nakagawa, *Nature* **417**, 601 (2002).
- [60] T. Bresler, M. Shapira, T. Boeckers, T. Dresbach, M. Futter, C. C. Garner, K. Rosenblum, E. D. Gundelfinger, and N. E. Ziv, *J. Neurosci* **24**, 1507 (2004).
- [61] M. V. Ehrensperger, C. Hanus, C. Vannier, A. Triller, and M. Dahan, *Biophys. J.* **92**, 3706 (2007).
- [62] A. E. El-Husseini, S. E. Craven, D. M. Chetkovich, B. L. Firestein, E. Schnell, C. Aoki, and D. S. Brecht, *J. Cell. Biol.* **148**, 159 (2000).
- [63] Ael-D. El-Husseini, E. Schnell, S. Dakoji, N. Sweeney, Q. Zhou, O. Prange, C. Gauthier-Campbell, A. Aguilera-Moreno, R. A. Nicoll, and D. S. Brecht, *Cell* **108**, 849 (2002).
- [64] C. Hanus, C. Vannier, and A. Triller, *J. Neurosci.* **24**, 1119 (2004).
- [65] C. Hanus, C. Vannier, and A. Triller, *J. Neurosci.* **24**, 1119 (2004).
- [66] A. Triller and D. Choquet, *Neuron* **59**, 359 (2008).